Supplemental Methods

Culture and induced maturation of HUDEP-2 cells

Mycoplasma-free HUDEP-2 cells were cultured as described previously[1]. Immature cells were expanded in the StemSpan serum-free medium (SFEM; STEMCELL Technologies) supplemented with 1 μM dexamethasone, 1 μg/mL doxycycline, 50 ng/mL human stem cell factor (SCF), 3 units/mL erythropoietin (EPO), and 1% penicillin–streptomycin. To induce erythroid maturation, HUDEP-2 cells were cultured in a differentiation medium composed of IMDM base medium (Invitrogen) supplemented with 2% FBS, 3% human serum albumin, 3 units/mL EPO, 10 μg/mL insulin, 1000 μg/mL holo-transferrin, and 3 units/mL heparin. Erythroid maturation was monitored by flow cytometry, using FITC-conjugated anti-CD235a (BD Biosciences, clone GA-R2), APC-conjugated anti-Band3 (from New York Blood Center), and Violet Blue–conjugated anti-CD49d (Miltenyi Biotec, clone MZ18-24A9) antibodies. $Band3^+$ and $Band3^-$ cell populations from the $CD235a^+$ cell fraction was purified by fluorescence-activated cell sorting (FACS).

Next generation DNA sequence analysis of HUDEP-2 cells for CRISPR/Cas9 sgRNA library screens

Library preparation and deep sequencing were performed as previously described[2,3]. Briefly, genomic DNA was extracted using a DNeasy Blood and Tissue kit (Qiagen). PCR amplicons were generated using lentiGuide-Puro specific primers that included a handle sequence. A second PCR amplification was performed using handle-specific primers to add adaptors and indexes to each sample. PCR products were analyzed on an agarose gel, and the DNA band of the expected size was excised and purified, then subjected to MiSeq 250-bp paired-end sequencing (Illumina) was performed. All PCR primers used are listed in Supplementary Table 11.

For data analysis, FastQ files obtained after MiSeq sequencing were demultiplexed using the MiSeq Reporter software (Illumina). Paired reads were trimmed and filtered using the CLC

Genomics Workbench (Qiagen) and matched against sgRNA sequences within the library. The read counts for each sgRNA were normalized against the total read counts across all samples. For each sgRNA, a *P* value (by paired two-tailed Student's *t*-test) and $\log_2$ fold change for enrichment were calculated for two groups of three matching samples and visualized using Spotfire (TIBCO). Gene ranking was based on the average fold difference in the representation of four individual corresponding sgRNAs in immature versus mature HUDEP-2 cells. A *P* of less than 0.05 was considered to indicate statistical significance. In addition, MAGeCK and MAGeCKFlute packages were further used to visualize the screening datasets and EnrichR was used for the GO analysis[4–6].

CRISPR/Cas9-mediated genome editing and gene knockdown in HUDEP-2 cells

The sgRNA sequences were selected from the CRISPR library or by using a CRISPR design tool (http://www.crisprscan.org/) and generated as oligonucleotides. After annealing, constructs were cloned into the *Bbs*I or *Bsm*BI site of the pXPR_003 vector or the plenti-V3_cherry vector (homemade), which encodes the sgRNA, Cas9, and GFP in a single vector, as shown in a previous study[7]. Oligonucleotides encoding short hairpin RNA (shRNA) constructs were designed by the RNAi Consortium of the Broad Institute, obtained from IDT, and cloned into the lentiviral vector pLKO.1-GFP, as previously described[8]. Luciferase shRNA-encoding pLKO.1–GFP (shLuc) was used as a control. The oligonucleotides encoding sgRNAs and shRNAs are listed in Supplemental Table 11.

For cell pool genome editing, HUDEP-2 cells stably expressing Cas9 were transduced with a lentiviral vector (pXPR_003) encoding individual sgRNAs. Cells were incubated for 7–10 days with 10 μg/mL blasticidin and 1 μg/mL puromycin to select for transduction with sgRNA and Cas9 vectors, respectively. To generate single gene–edited clones, 1×10^6 cells were electroporated with 10 μg of plasmid encoding sgRNA, Cas9, and GFP in the OE1 vector. After

24 hour of transduction, single GFP^+ cells were sorted into 96-well plates and expanded for 14–21 days. To enrich for genomic DNA, cells were incubated in DNA extraction buffer (100 mM Tris-HCl, pH 8.3; 200 mM NaCl; 5 mM EDTA; 1% Triton X-100; 200 µg/mL proteinase K) at 50°C for 1 h and then at 85°C for 30 min. On-target insertion/deletion mutations were characterized by PCR amplification, followed by next-generation sequencing and then by CRISPResso2 analysis[9].

To introduce an in-frame C-terminal V5 tag sequence into the endogenous *BAHD1* gene, sgRNAs were designed with at least 3 bp of mismatch to any other site in the human genome to mitigate the risk of off-target editing. Approximately 500,000 HUDEP2 cells were transiently co-transfected with 0.5 µg of pmaxGFP plasmid (Lonza), 33 pmol of spCas9 protein, 100 pmol of chemically modified sgRNA (Synthego), and 100 pmol of ssODN (IDT) via nucleofection (with a Lonza, 4D-Nucleofector™ X-Unit), using solution P3 and program DS-150 in small (20-µL) cuvettes in accordance with the manufacturer's recommended protocol. Five days after nucleofection, cells were single-cell sorted into 96-well plates by FACs for transfected cells, based on the pmaxGFP expression into 96-well plates. Cells were clonally expanded, and the integration of the C-terminal V5 tag was verified via targeted deep sequencing followed by CRIS.py analysis[10]. All primers used are listed in Supplementary Table 11.

$CD34^+$ cell culture and manipulation

$CD34^+$ hematopoietic stem and progenitor cells (HSPCs) were mobilized from normal subjects by granulocyte colony-stimulating factor, collected by apheresis, and enriched by immunomagnetic bead selection using an autoMACS Pro Separator (Miltenyi Biotec), in accordance with the manufacturer's protocol. At least 95% purity was achieved, as assessed by flow cytometry using a PE-conjugated anti-human CD34 antibody (Miltenyi Biotec, clone AC136, catalog #130-081-002). A three-phase culture protocol was used to promote erythroid differentiation and

maturation[11]. In phase 1 (days 0–7), cells were cultured at a density of 10^5–10^6 cells/mL in IMDM with 2% human AB plasma, 3% human AB serum, 1% penicillin/streptomycin, 3 IU/mL heparin, 10 μg/mL insulin, 200 μg/mL holo-transferrin, 1 IU EPO, 10 ng/mL SCF, and 1 ng/mL IL-3. In phase 2 (days 8–12), IL-3 was omitted from the medium. In phase 3 (days 12–18), cells were cultured at a density of 10^6/mL, with both IL-3 and SCF being omitted from the medium and the holo-transferrin concentration being increased to 1 mg/mL. Erythroid differentiation and maturation were monitored by flow cytometry, using FITC-conjugated anti-CD235 (BD Biosciences, clone GA-R2, catalog #561017), APC-conjugated anti-Band3 (homemade), and Violet Blue–conjugated anti-CD49d (Miltenyi Biotec, clone MZ18-24A9, catalog #130-099-680) antibodies.

Myeloid differentiation: A total of 1×10^4 $CD34^+$ cells (in a volume of 1 mL) were seeded into each well of a 12-well plate (1 mL/well) and cultured in SFEM II supplemented with StemSpan Myeloid Expansion Supplement (STEMCELL Technologies, catalog #02693). Every 2 days, 500 μL of fresh medium was added. Cells were collected by centrifugation (300 × g, 5 min) and resuspended in fresh medium every 7 days. Cells were analyzed by flow cytometry on days 7 and 14 for expression of myeloid lineage markers, using BV421-conjugated anti-CD33 (BD Bioscience, clone HIM3-4, catalog #744350) and APC-conjugated anti-CD11b (BD Bioscience, clone ICRF44, catalog #550019) antibodies.

Megakaryocyte differentiation: A total of 1×10^4 $CD34^+$ cells (in a volume of 1 mL) seeded into each well of a 12-well plate (1 mL/well) and cultured in SFEM II plus StemSpan Megakaryocyte Expansion Supplement (STEMCELL Technologies, catalog #02696). Every 2 days, 500 μL of fresh medium was added. Cells were centrifuged and resuspended in fresh medium every 7 days. On days 14 and 28, cells were analyzed for the expression of megakaryocyte lineage

markers, by using PE-Cy7–conjugated anti-CD41a (BD Bioscience, clone HIP8, catalog #561424) and APC-conjugated anti-CD42b (BD Bioscience, clone HIP1, catalog #551061) antibodies.

Methylcellulose colony assays: $CD34^+$ cells were cultured for 24 h in expansion medium (StemSpan SFEM with 100 ng/mL hSCF, 100 ng/mL Flt3-L, and 50 ng/mL TPO), and then seeded at 300 cells/mL into full cytokine human methylcellulose (STEMCELL Technologies; 300 cells/3-cm dish). Colonies were quantified after 2 weeks of culture.

Lentiviral vector transduction: A total of 2×10^5 $CD34^+$ cells were resuspended in 200 µL of phase I medium with concentrated vector (at a MOI of approximately 0.3) and 8 µg/mL polybrene. Cells were collected by centrifugation at $800 \times g$ for 90 min at 37°C. At 48 h after transduction, transduced cells were enriched for selectable markers by FACS for GFP^+ cells. GFP^+ cells were then induced for further culture experiments.

Gene disruption by CRISPR/Cas9: Cas9-sgRNA ribonucleoproteins (RNPs) were generated by incubating 5 µg of purified Cas9 (from the University of California, Berkeley) with sgRNAs (at a molar ratio of 1:2) in a total volume of 5 µL in HF-150 buffer at room temperature for 25 mins. The RNP cocktail was mixed with 2×10^5 $CD34^+$ cells in a total volume of 20 µL in T buffer, then the cells were electroporated under these conditions with three pulses of 1600 V for 10 ms each, using a Neon Transfection System 10 µL kit (Thermo Fisher Scientific, catalog #MPK1096). After electroporation, the cells were transferred to the culture medium for further analysis.

Cytocentrifuge preparations: Approximately 50,000–200,000 cells were washed in PBS, resuspended in 200 µL of FACS buffer (0.5% bovine serum albumin [BSA] in PBS), and deposited onto poly-L-lysine–coated microscope slides, using a Shandon 4 cytocentrifuge (Thermo Fisher Scientific) at 300 rpm for 4 min. Dried slides were fixed and stained with May–Grünwald solution (Sigma–Aldrich) for 5 min, rinsed four times in deionized water, and stained in Giemsa solution

(Sigma–Aldrich) for 15 min. Slides were washed in water and dried, then coverslips were mounted. All images were acquired with AxioVision software (Zeiss) at 60× magnification.

RNA sequencing

For RNA-seq, RNA was extracted from 5×10^6 HUDEP-2 cells (with at least three biological replicates in each case) by using a RNeasy Mini kit (Qiagen). A TruSeq Stranded mRNA Library Prep Kit (Illumina) was used to enrich for polyA+ RNA and create libraries for sequencing with a HiSeq2000 System (Illumina). RNA-seq reads were aligned to the hg19 human genome by using the StrongARM pipeline[12]. The htseq-count script (HTSeq framework, version 0.6.1p1)[13] was used to annotate associated aligned reads to the human genome, and NCBIM37.67 was used to obtain per-gene counts. Hemoglobin and small nucleolar RNAs were excluded from the analysis. All differentially expressed transcripts were selected using a cutoff of $P < 0.05$. For the histone features analysis, transcripts with an absolute value of $\log_2$ fold change greater than 1.0 and expression higher than one transcript per million reads under at least one condition were considered to be significantly differentially expressed.

Quantitative proteomics (10-plex TMT-LC/LC-MS/MS)

Protein sample preparation: To prepare protein samples, 10^7 HUDEP-2 cells for each sample were washed with PBS; lysed in 50 mM HEPES, pH 8.5, 8 M urea; and centrifuged at 15,000 × *g* for 5 mins. Protein concentrations in the supernatant were quantified by the BCA protein assay (Thermo Fisher Scientific) and confirmed by SDS polyacrylamide gel electrophoresis (PAGE) with titrated BSA concentrations, followed by Coomassie staining[14]. For each sample, 100 µg was digested with Lys-C (Wako; 1:100 w/w) at room temperature for 2 h; diluted 4-fold with 50 mM HEPES, pH 8.5; and further digested with trypsin (Promega; 1:50 w/w)

at room temperature overnight. The resulting peptides were acidified by adding trifluoroacetic acid to a concentration of 1% and, then the preparation was centrifuged at 21,000 × *g* for 10 mins to remove debris. The supernatant was desalted with a Sep-Pak C18 cartridge (Waters), eluted with 60% acetonitrile plus 0.1% trifluoroacetic acid, and dried with a SpeedVac concentrator. Each sample was then resuspended in 50 mM HEPES and labeled with tandem mass tag (TMT) 10plex reagents (Thermo Fisher Scientific) in accordance with the manufacturer's instructions. Samples labeled with different tags were mixed at a 1:1 (w/w) ratio, desalted, and dried with a SpeedVac.

Offline basic pH reversed-phase liquid chromatography: Mixed TMT-labeled peptides were solubilized in buffer A (10 mM ammonium formate, pH 8.0) and separated on an XBridge C18 column (3.5-μm particle size, 4.6-mm i.d., 25-cm length; Waters). The sample was separated into 80 fractions, using a 2-h gradient from 15% to 35% buffer B (95% acetonitrile, 10 mM ammonium formate, pH 8.0). A total of 38 fractions (i.e., every other fraction) were collected, dried, and reconstituted for liquid chromatography–tandem mass spectrometry (LC-MS/MS) analysis[15].

Acidic pH reversed-phase liquid chromatography coupled with tandem MS: The LC-MS/MS analysis was performed using an optimized platform[16]. Dried peptides were analyzed on an Orbitrap Fusion Tribrid mass spectrometer (Thermo Fisher Scientific) after separation on a 40 cm × 75 μm i.d. column packed with 1.9-μm C18 resin (Dr. Maisch GmbH, Germany). Separation was achieved by applying a 2-hours 10%–40% buffer B gradient (buffer A: 0.2% formic acid, 5% DMSO; buffer B: buffer A plus 65% acetonitrile). The column was heated to 65°C with a Butterfly Portfolio Heater (Phoenix S&T) to reduce backpressure. MS was performed in a data-dependent mode with a survey scan in Orbitrap (60,000 resolution, 2×10^5 automatic gain control target, and 50-ms maximal ion time). During data-dependent acquisition, Orbitrap survey spectra were scheduled for execution at least every 3s, with the embedded control system determining the

number of MS/MS acquisitions executed during this period. Parameters for MS/MS scans were HCD, 1×10^5 AGC target, 150-ms maximal ion time, 1-m/z isolation window, of 38 normalized collision energy, and 20-s dynamic exclusion.

Data analyses: Data were processed by the JUMP algorithm as previously reported[17,18]. Briefly, MS/MS raw files were converted into the mzXML format and searched by the JUMP algorithm against a composite target/decoy database to estimate the FDR. The target protein database was downloaded from the UniProt mouse database, and the decoy protein database was generated by reversing all target protein sequences. Spectra were searched with ±10 ppm for precursor ion and product ion mass tolerance, fully tryptic restriction, static mass shift for TMT-tagged N-terminus and lysine (+229.16293), dynamic modification for oxidation (+15.99492) of methionine, two maximal missed cleavages, and the assignment of a, b, and y ions. Putative peptide spectra matches were filtered to an FDR lower than 1%. Proteins were quantified by the TMT reporter ion intensities of each peptide-spectrum match of its identified peptides.

Combined RNA-seq/proteomic analysis for FBXO11 substrate identification

Protein IDs from MS data were mapped to gene symbols by using HUMAN_10090_idmapping.dat and uniprotHuman.tab from the UniProt database (http://www.uniprot.org/) as downloaded on 9/24/2015. Data corresponding to samples with matched identities by RNA-seq and proteomic analysis were analyzed using the R statistical environment. Counts were normalized using voom[19], and differential expression analysis was performed using LIMMA[20]. For Figure 3e, the $\log_2$ fold changes between WT and *FBXO11* knockout HUDEP-2 cell pools were plotted for 9,231 proteins from quantitative proteome analysis and for 14,642 mRNAs from RNA-seq analysis. Traditional and robust linear regression analyses were conducted to fit the $\log_2$ fold change in mRNA and protein. The correlation data shown in Fig. 3e ($R = 0.522$) are based on the robust linear regression

model. Residuals calculated based on linear regression and robust linear regression were used to detect outliers, thereby indicating the potential substrates, identified as those with a > 1.6-fold increase in protein expression F11KO cells ($\log_2$ fold change ≥ 0.7, $P < 0.05$) and a minimal change in the corresponding mRNA ($\log_2$ fold change ≤ 0.5). All analyses were conducted in R-3.3.1.

Isolation of nuclear and cytoplasmic fractions from HUDEP-2 cells

The method was adapted from a previous study of B cells[21]. In brief, the freshly prepared cell pellet (containing approximately 10^7 cells) was gently resuspended in Buffer 1 (0.32 M sucrose, 3 mM $CaCl_2$, 2 mM magnesium acetate, 10 mM Tris [pH 8], 0.1 mM EDTA, 0.5% NP40, with freshly added 1 mM DTT, 1 mM PMSF, and 1× protease inhibitor cocktail). After centrifugation at $500 \times g$ for 5 min at 4˚C, the supernatant was collected: this was the cytoplasmic fraction. The remaining nuclei were washed once with 1 mL of Buffer 1 lacking NP-40 and then lysed with 122 µL/10^7 cells of high salt buffer (10 mM Tris [pH 7.5], 2 mM MgCl2, 1% Triton X, 400 mM NaCl, 1 mM PMSF, 1× protease inhibitor cocktail). After incubation on ice for 15 min and further centrifugation at 14,000 rpm for 10 min, the supernatant representing the nuclear extract was collected. The remaining pellet was washed once with high-salt buffer, then 1% SDS buffer (50 mM Tris [pH 7.5], 150 mM NaCl, 0.5% NP40, 1% SDS, 1 mM EDTA, 1 mM PMSF, 1× protease inhibitor cocktail) was added, followed by sonication at a high setting, on ice. Sonication was performed three times, resulting in a suspension of insoluble chromatin material. Four-X SDS loading buffer (Invitrogen, catalog #NP0007) was added to the cell fractions and they were boiled for 10 min before Western blotting was performed.

Western blot analysis

Cells were suspended in Pierce IP Lysis Buffer (Thermo Fisher Scientific, catalog #87787) supplemented with 1 mM phenylmethylsulfonyl fluoride and 1:500 protease inhibitor cocktail (Sigma–Aldrich). Proteins were resolved on polyacrylamide gels (Bio-Rad), transferred to a PVDF membrane, and incubated in blocking buffer (5% non-fat milk in TBST). Antibody staining was visualized using the Odyssey CLx Imaging System. For BAHD1 Western blotting, the primary antibody (Abcam, catalog #ab46573) was diluted 1:500 in blocking buffer (to a final concentration of 2 μg/mL). The secondary antibody (goat anti-rabbit IgG [H+L] with HRP; Invitrogen, catalog #31460) was diluted 1:2000 in blocking buffer (to a final concentration of 0.4 μg/mL). The SuperSignal™ West Femto Maximum Sensitivity Substrate (Thermo Fisher Scientific, catalog #34094) was used for antibody signal detection. The antibodies used for Western blot analysis are listed in Supplemental Table 11.

Immunoprecipitation and immunofluorescence

The 293T cells were co-transfected with expression constructs encoding Myc or V5-tagged BAHD1 (full-length or truncated mutants) and FLAG-tagged FBXO11 in 10-cm plates, using Lipofectamine2000 (Invitrogen) in accordance with the manufacturer's instructions. After 48 h, the cells were treated with 15 μM MG132 for 4 hours, lysed in immunoprecipitation (IP) buffer (Thermo Fisher Scientific, catalog#87788) at 4°C for 30 mins, and centrifuged at 13,000 × g for 15 mins. The supernatants were collected, and immunoprecipitation was performed using anti-FLAG (Sigma–Aldrich, catalog #F3165), anti-Myc (Millipore, catalog #05-724), or anti-V5 (Thermo Fisher Scientific, catalog #R960-25) antibodies, as described previously[22,23]. Briefly, the cell lysate was precleared with Pierce Protein A/G magnetic beads (Thermo Fisher Scientific, catalog #88803) for 2 h then incubated with the antibody overnight. This was followed by incubation for 4 h with fresh Protein A/G magnetic beads. The beads were then washed three times

with IP buffer, and 2× SDS-PAGE sample buffer was added. Samples were boiled for 5 min then centrifuged, and the supernatants were subjected to Western blot analysis.

For immunofluorescence, sections were permeabilized with 0.1% Triton X-100 in PBS for 15 min at room temperature; treated with 3% BSA and 3% goat serum, 0.1% Triton, and 0.05% Tween-20 in PBS for 1 h; and then incubated with a primary antibody overnight at 4°C. Sections were then washed extensively, incubated with the secondary antibody for 2 h at room temperature, mounted on glass slides, and visualized with a confocal laser scanning microscope (Nikon Eclipse TE2000-E).

Protein–protein network analysis of the BAHD1 complex and the PRC2 complex

A composite protein-protein interactome was built by combining STRING (v10) [24], BioPlex[25], and InWeb[26] as described previously[17]. The significance of the BAHD1−PRC subnetworks was evaluated by empirically estimating the probability of observing a denser network by random sampling of 1,000 subnetworks from the entire interactome. The network was calculated using R–graph version 1.2.4.1[27].

Cycloheximide pulse-chase assay

Cycloheximide pulse-chase experiments were performed as described previously[22]. Cells were seeded into 6-well plates at 10^6 cells/mL, 1 mL/well, and incubated overnight. Then, 50 μg/mL of cycloheximide was added, and cells were collected serially for protein assessment by Western blot analysis.

***In vitro* ubiquitination assay**

Constructs, protein expression, and purification: Expression constructs were prepared by using standard molecular biology techniques, and coding sequences were entirely verified in their entirety. All protein sequences were from humans. UBC12, UBCH5B, APPBP1-UBA3 (NEDD8 E1), UBA1 (UB E1), CUL1–RBX1, NEDD8, and UB were expressed and purified as described previously[28]. Neddylation and purification of CUL1–RBX1 was performed as described previously[29]. SKP1–FBXO11$^{56\text{-}\Delta UBR}$ was prepared by expressing His–TEV–FBXO11 (residues 56–833) and SKP1 (coexpressed bicistronically from a homemade modified pRSFDuet vector) in *E. coli* BL21 gold cells. The expressed complex was purified by nickel affinity chromatography, and the complex was further purified over a HiTrap Q and Superdex SD200 gel filtration column. Fragments of BAHD1 were cloned as GST–TEV fusions in a modified pGEX vector and expressed in *E. coli*. Fusion proteins were purified by glutathione affinity chromatography, followed by cleavage with TEV protease to remove GST. BAHD1 fragments were further purified over a HiTrap S and Superdex SD75 gel filtration column.

Biochemical assays: The ubiquitination of BAHD1 fragments was monitored by pulse-chase assays to exclusively follow exclusively the transfer of fluorescently labeled ubiquitin from the E2 enzyme UBCH5B[30]. For the pulse reaction, the thioester-linked E2~UB intermediate was generated by incubating 10 µM UBCH5B, 15 µM fluorescent UB, 400 nM UBA1 in 25 mM HEPES, 200 mM NaCl, 2.5 mM $MgCl_2$, and 1 mM ATP, pH 7.5, for 15 min at room temperature. Pulse formation of the thioester-linked E2~UB intermediate was quenched with 50 mM EDTA on ice for 5 min. SCF^{FBXO11} complexes were equilibrated on ice for 30 min before initiating the chase reactions were initiated by mixing the components to a final concentration of 0.25 µM Nedd8-modified RBX1–CUL1, 0.375 µM SKP1–FBXO11$^{56\text{-}\Delta UBR}$, and 2.5 µM of the indicated BAHD1 fragment in 50 mM HEPES, 100 mM NaCl, pH 7.5. Chase reactions were performed at room temperature by diluting the thioester-linked UBCH5B~UB intermediate to 0.125 µM in 50 mM

HEPES, 100 mM NaCl, 50 mM EDTA, 0.5 mg/mL BSA, pH 7.5, followed by the addition of the SCF complex mixture to a final concentration of 0.1 μM. Aliquots were removed at the indicated times and quenched with 2× SDS-PAGE sample buffer. The reaction products were separated and visualized as described above.

ChIP-sequencing library preparation and data analysis

ChIP experiments were performed as previously described[31] with at least two biological replicates for each study. First, 20×10^6 HUDEP-2 cells were suspended in 50 mL of PBS. Then, cells were cross-linked for 10 min with formaldehyde (1% final concentration) in a shaker at room temperature, quenched with 0.125 M glycine for 5 min, washed in PBS, and lysed in 20 mL of cell lysis buffer (Chromatin L1) containing protease inhibitors for 10 min at 4°C. Lysates were centrifuged at $800 \times g$ for 10 min, then the cell pellets were resuspended in 20 mL of nuclei lysis buffer (Chromatin L2) containing protease inhibitors. The cells were incubated for 10 min at 4°C, then collected by centrifugation at $800 \times g$. Cell pellets were resuspended in 2 mL of RIPA buffer and sonicated for 12 cycles (10 s on/90 s off with 20% output from a Branson 250 Sonifier with a micro-tip probe for a total pulse time of 2 min). Sonicated chromatin was centrifuged at $18,000 \times g$ at 4°C for 15 min. Supernatants were precleared by incubating them with 200 μL of Protein A/G agarose bead slurry (Thermo Fisher Scientific, catalog #15918014) overnight at 4°C with rotation, followed by centrifugation to remove the beads. Separately, 10 μg of IP antibody was incubated with 50 μL of Protein A/G agarose bead slurry in 1 mL of PBS overnight at 4°C with rotation. Saved precleared chromatin (50 μL) was used as the input sample. Precleared chromatin was incubated with the antibody–bead complex for 4 h at 4°C with rotation, and immunocomplexes were washed as follows: once with IP wash I buffer (20 mM Tris-Cl, pH 8.0; 2 mM EDTA; 50 mM NaCl; 1% Triton X-100; 0.1% SDS), twice with high-salt buffer (20 mM Tris-Cl, pH 8.0; 2

mM EDTA; 500 mM NaCl; 1% Triton X-100; 0.01% SDS), once with IP wash II buffer (10 mM Tris-Cl, pH 8.0; 1 mM EDTA; 0.25 mM LiCl: 1% NP-40; 1% sodium deoxycholate), and twice with TE, pH 8.0. Washed immunocomplexes were eluted from beads by incubation with 200 µL of elution buffer (1% SDS, 0.1 M $NaHCO_3$) at 45°C for 30 min. Cross-links were reversed by incubation with RNaseA (1 µg/µL) and 0.25 M NaCl overnight at 65°C, followed by treatment with proteinase K (0.2 mg/mL) for 2 h at 45°C. Immunoprecipitated DNA was purified using a QIAgen PCR Extraction Kit and eluted with 20 µL of EB elution buffer.

Library construction: ChIP-seq libraries were constructed using the NEBNext Ultra II DNA Library Prep Kit for Illumina (New England BioLabs, catalog #E7645) in accordance with the manufacturer's instructions. Briefly, 20 µL of purified ChIP DNA was end repaired for dA tailing, followed by adaptor ligation. Adaptor-ligated ChIP DNA was size selected with SPRI clean-up by AMPure XP beads (1:1 ratio) twice. Then, ChIP DNA was used for 7–15 cycles of PCR amplification and the products were purified with a MinElute column (Qiagen, catalog #28006), using the MinElute PCR Purification Kit and protocol. Finally, DNA was size selected (350–600 bp) by agarose gel electrophoresis and extracted from the gel with a QIAquick Gel Extraction Kit (Qiagen). The quality of the ChIP-seq library was determined with an Agilent 2100 Bioanalyzer, using the High-Sensitivity Chip (Agilent). The average sizes of the ChIP-seq libraries ranged from 350 to 600 bp. For multiplexing, equal molar quantities of libraries were combined by considering the sequencing depth per sample (40 million reads per library). ChIP-seq libraries were sequenced using an Illumina HiSeq2500 System or a NextSeq platform with single-end reads of 50 bases.

Data analysis: Short reads from ChIP-seq experiments were mapped to the human reference genome hg19, by using BWA version 0.7.12. Multiple mapped reads and duplicated reads were filtered out after mapping. For each experiment, fragment lengths were estimated based

on the cross-correlation plot, using SPP (v1.11) for each experiment, which was also used for peak calling. After quality control[32] according to ENCODE guidelines, filtered alignments were fed into MACS2 (v2.1.1.20160309) for peak calling of the point-source factor (H3K4me3) and broad peak factors (BAHD1, H3K27me3). Peaks were called twice for each sample with FDR-corrected *P*-value cutoffs of 0.05 (the high confidence peak) and 0.5 (the low confidence peak), and reproducible peaks were finalized by requiring a peak called in high confidence of any replicate to also overlap low confidence peaks from all other replicates. For BAHD1 and H3K27me3, SICER (V1.1) peaks were also called and reproducible peaks not overlapping MACS2 peaks were merged into MACS2 finalized peaks. Known false-positive peaks recorded in the ENCODE blacklist were removed from the final peak list.

For visualization, reads were extended to the fragment size estimated by SPP and normalized to 15M non-duplicated reads to generated bigwig files. Deeptools (v2.5.7) was used to plot the heatmap average in 10-bp bins. The color scale of the heatmap for each histone mark was manually set to fit the value into the best range. Peak categorization with respect to gene structure: a. the promoter, within 2 kb upstream and downstream of the TSS; b. the 5′ distal region, from 50 kb upstream of the TSS to 2 kb upstream of the TSS; c. exons, all exons in the gene body from the TSS to the TES; d. introns, all introns in the gene body from the TSS to the TES; e. the TES, within 2 kb upstream and downstream of the TES; f. the 3′ distal region: from 2 kb downstream of the TES to 50 kb downstream of the TES; g. the intergenic region, >50 kb upstream of the TSS and >50 kb downstream of the TES. To analyze GATA1 binding in HUDEP-2 cells, we determined the H3K27me3 peak distribution around the TSS in genes with decreased expression after *FBXO11* knockout. The average peak width at the TSS (± 2 standard deviations) was approximately 9.8 kb. Thus, we quantified GATA1 ChIP-seq signals within a 10-kb region centered on the TSS.

ATAC-seq library preparation and data analysis

The ATAC-seq library was prepared according to the published omni-ATAC protocol, using 50,000 live cells per sample[33]. Libraries were pair-end 100-bp sequenced using an Illumina HiSeq 4000 System. They then underwent trimmed adaptor sequencing and were mapped to hg19 by using BWA. Reads mapped to mitochondrial DNA were removed. The 2 × 100-bp paired-end reads obtained from all samples were trimmed for Nextera adapters by cutadapt (version 1.9, paired-end mode, default parameter with " –m 6 –O 20 ") and aligned to human genome hg19(GRCh37-lite) by BWA (version 0.7.12-r1039, default parameter)[34]. Duplicated reads were then marked with Picard (version 2.6.0-SNAPSHOT), and only non-duplicated proper paired reads were kept by SAMtools (parameter "-q 1 -F 1804," version 1.2)[35]. After adjusting the Tn5 shift (reads were offset were offset by +4 bp for the sense strand and by −5 bp for the antisense strand), we separated the reads into nucleosome-free, mononucleosome, dinucleosome, and trinucleosome categories, as described[36] , based on fragment size and generated bigwig files by using the center 80 bp of fragments and scaling to 30M nucleosome-free reads. We observed reasonable nucleosome-free peaks and patterns of mono-, di-, tri-nucleosomes on IGV (version 2.4.13)[37]. Next, we merged each pair of replicates to enhance peak calling on nucleosome-free reads, with all samples achieving approximately 10M nucleosome free reads. We then called peaks by MACS2(version 2.1.1.20160309; default parameters with "--extsize 200 –nomodel") [38]. To ensure the replicability, we counted nucleosome-free reads from each of the samples by using BEDTools (v2.24.0)[39]. We observed the Pearson correlation coefficient to be greater between replicates (> 0.80 for most) than between samples from two different groups. To identify differential accessible regions, we first normalized raw nucleosome-free reads counts, using the trimmed mean of M-values normalization method, and applied the empirical Bayes statistics test after linear fitting from the voom package (R 3.23, edgeR 3.12.1, limma 3.26.9)[19]. An FDR-corrected *P* value of 0.05 and

a fold change greater than 2 were used as cutoffs for more accessible regions in FBXO11 KO (Gain region) or less accessible regions in FBXO11 KO (Loss region) compared to wild type HUDEP-2 cells. For motif analysis, we selected regions with a fold change of less than 0.05 and a *P* value of less than 0.5 as control regions. FIMO from the MEME suite (version 4.11.3, "--thresh 1e-4 --motif-pseudo 0.0001")[40] was used for scanning motif (using the TRANSFAC database, which includes only vertebrata and is not 3D structure-based) matches in the nucleosome-free regions, and Fisher's exact tests were used to test whether a motif was significantly enriched for differentially accessible regions, as compared to the control regions.

All statistical calculations were performed using GraphPad Prism. A two-tailed, unpaired Student's *t*-test was used for comparisons between two groups. Data are presented as the mean ± SEM, with *P* values of less than 0.05 being considered to indicate significance. Gene set enrichment analysis and Gene Ontology analyses were conducted according to the default parameters in their native implementations. Fisher's exact test was used for statistical enrichment of gene lists. No statistical methods were used to predetermine sample size.

REFERENCES

1. Kurita R, Suda N, Sudo K, et al. Establishment of immortalized human erythroid progenitor cell lines able to produce enucleated red blood cells. *PLoS One*. 2013;8(3):e59890.
2. Shalem O, Sanjana NE, Hartenian E, et al. Genome-scale CRISPR-Cas9 knockout screening in human cells. *Science.* 2014;343(6166):84–87.
3. Wang T, Lander ES, Sabatini DM. Single guide RNA library design and construction. *Cold Spring Harb. Protoc.* 2016;2016(3):283–288.
4. Kuleshov M V., Jones MR, Rouillard AD, et al. Enrichr: a comprehensive gene set enrichment analysis web server 2016 update. *Nucleic Acids Res.* 2016;44(W1):W90–W97.
5. Li W, Xu H, Xiao T, et al. MAGeCK enables robust identification of essential genes from genome-scale CRISPR/Cas9 knockout screens. *Genome Biol.* 2014;15(12):554.
6. Wang B, Wang M, Zhang W, et al. Integrative analysis of pooled CRISPR genetic screens using MAGeCKFlute. *Nat. Protoc.* 2019;14(3):756–780.

7. Traxler EA, Yao Y, Wang YD, et al. A genome-editing strategy to treat β-hemoglobinopathies that recapitulates a mutation associated with a benign genetic condition. *Nat. Med.* 2016;22(9):987–990.

8. Sancak Y, Peterson TR, Shaul YD, et al. The Rag GTPases bind raptor and mediate amino acid signaling to mTORC1. *Science.* 2008;320(5882):1496–1501.

9. Clement K, Rees H, Canver MC, et al. CRISPResso2 provides accurate and rapid genome editing sequence analysis. *Nat. Biotechnol.* 2019;37(3):224-226.

10. Connelly JP, Pruett-Miller SM. CRIS.py: a versatile and high-throughput analysis program for CRISPR-based genome editing. *Sci. Rep.* 2019;9(1):4194.

11. Giani FC, Fiorini C, Wakabayashi A, et al. Targeted application of human genetic variation can improve red blood cell production from stem cells. *Cell Stem Cell*. 2016;18(1):73–78.

12. Pinto EM, Chen X, Easton J, et al. Genomic landscape of paediatric adrenocortical tumours. *Nat. Commun.* 2015;6:6302.

13. Anders S, Pyl PT, Huber W. HTSeq—a Python framework to work with high-throughput sequencing data. *Bioinformatics*. 2015;31(2):166–169.

14. Xu P, Duong DM, Peng J. Systematical optimization of reverse-phase chromatography for shotgun proteomics. *J. Proteome Res.* 2009;8(8):3944–3950.

15. Bai B, Tan H, Pagala VR, et al. Deep profiling of proteome and phosphoproteome by isobaric labeling, extensive liquid chromatography, and mass spectrometry. *Methods Enzymol.* 2017;585:377–395.

16. Wang H, Yang Y, Li Y, et al. Systematic optimization of long gradient chromatography mass spectrometry for deep analysis of brain proteome. *J. Proteome Res.* 2015;14(2):829–838.

17. Tan H, Yang K, Li Y, et al. Integrative proteomics and phosphoproteomics profiling reveals dynamic signaling networks and bioenergetics pathways underlying T cell activation. *Immunity*. 2017;46(3):488–503.

18. Wang X, Li Y, Wu Z, et al. JUMP: a tag-based database search tool for peptide identification with high sensitivity and accuracy. *Mol. Cell. Proteomics*. 2014;13(12):3663–3673.

19. Law CW, Chen Y, Shi W, Smyth GK. voom: precision weights unlock linear model analysis tools for RNA-seq read counts. *Genome Biol.* 2014;15(2):R29.

20. Ritchie ME, Phipson B, Wu D, et al. Limma powers differential expression analyses for RNA-sequencing and microarray studies. *Nucleic Acids Res.* 2015;43(7):e47.

21. Dyer RB, Herzog NK. Isolation of intact nuclei for nuclear extract preparation from a fragile B-lymphocyte cell line. *Biotechniques*. 1995;19(2):192–195.

22. Rossi M, Duan S, Jeong YT, et al. Regulation of the CRL4(Cdt2) ubiquitin ligase and cell-cycle exit by the SCF(Fbxo11) ubiquitin ligase. *Mol. Cell*. 2013;49(6):1159–1166.

23. Horn M, Geisen C, Cermak L, et al. DRE-1/FBXO11-dependent degradation of BLMP-1/BLIMP-1 governs C. elegans developmental timing and maturation. *Dev. Cell*. 2014;28(6):697–710.

24. Szklarczyk D, Franceschini A, Wyder S, et al. STRING v10: protein–protein interaction networks, integrated over the tree of life. *Nucleic Acids Res.* 2015;43(D1):D447–D452.

25. Huttlin EL, Ting L, Bruckner RJ, et al. The BioPlex network: a systematic exploration of the human interactome. *Cell*. 2015;162(2):425–440.

26. Li T, Wernersson R, Hansen RB, et al. A scored human protein-protein interaction network to catalyze genomic interpretation. *Nat. Methods*. 2016;14(1):61–64.

27. Csardi G, Nepusz T. The igraph software package for complex network research. *InterJournal Complex Syst.* 2006;1695.

28. Scott DC, Rhee DY, Duda DM, et al. Two distinct types of E3 ligases work in unison to regulate substrate ubiquitylation. *Cell*. 2016;166(5):1198–1214.e24.

29. Duda DM, Borg LA, Scott DC, et al. Structural insights into NEDD8 activation of Cullin-RING ligases: conformational control of conjugation. *Cell*. 2008;134(6):995–1006.

30. Scott DC, Sviderskiy VO, Monda JK, et al. Structure of a RING E3 trapped in action reveals ligation mechanism for the ubiquitin-like protein NEDD8. *Cell*. 2014;157(7):1671–1684.

31. Landt SG, Marinov GK, Kundaje A, et al. ChIP-seq guidelines and practices of the ENCODE and modENCODE consortia. *Genome Res.* 2012;22(9):1813–1831.

32. Wang L, Hiler D, Xu B, et al. Retinal cell type DNA methylation and histone modifications predict reprogramming efficiency and retinogenesis in 3D organoid cultures. *Cell Rep.* 2018;22(10):2601–2614.

33. Corces MR, Trevino AE, Hamilton EG, et al. An improved ATAC-seq protocol reduces background and enables interrogation of frozen tissues. *Nat. Methods*. 2017;14(10):959–962.

34. Li H, Durbin R. Fast and accurate short read alignment with Burrows-Wheeler transform. *Bioinformatics*. 2009;25(14):1754–1760.

35. Li H, Handsaker B, Wysoker A, et al. The Sequence Alignment/Map format and SAMtools. *Bioinformatics*. 2009;25(16):2078–2079.

36. Buenrostro JD, Giresi PG, Zaba LC, Chang HY, Greenleaf WJ. Transposition of native chromatin for fast and sensitive epigenomic profiling of open chromatin, DNA-binding proteins and nucleosome position. *Nat. Methods*. 2013;10(12):1213–1218.

37. Robinson JT, Thorvaldsdóttir H, Winckler W, et al. Integrative genomics viewer. *Nat. Biotechnol.* 2011;29(1):24–26.

38. Zhang Y, Liu T, Meyer CA, et al. Model-based analysis of ChIP-Seq (MACS). *Genome Biol.* 2008;9(9):R137.

39. Quinlan AR, Hall IM. BEDTools: a flexible suite of utilities for comparing genomic features. *Bioinformatics*. 2010;26(6):841–842.

40. Bailey TL, Boden M, Buske FA, et al. MEME Suite: tools for motif discovery and searching. *Nucleic Acids Res.* 2009;37(W):W202–W208.

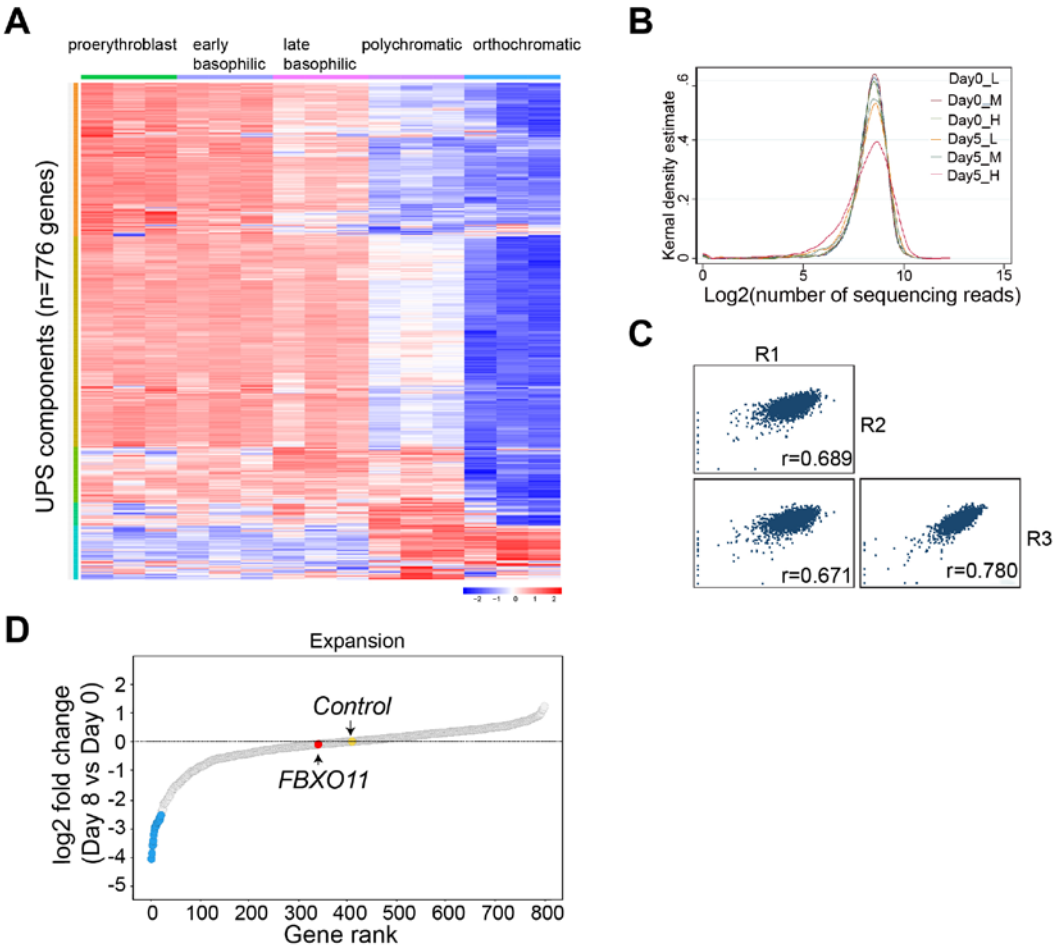

Supplemental Figure 1 (related to Figure 1). Single-guide (sg) RNA screen for ubiquitin–proteasome system (UPS) genes that facilitate erythroid maturation.

(A) Heatmap showing the expression of 776 UPS genes at specific stages of erythroid maturation. The original data from a previous study were processed[1]. The expression values of genes differentially expressed between stages of maturation are organized by agglomerative hierarchical clustering.

(B) Representation of pooled library sgRNAs in fractionated cell populations at days 0 and 5 of cell culture under erythroid maturation conditions. H, M, and L refer to high, median, and low Band3 expression in cells purified by flow cytometry. The median was approximately 300 normalized reads. The x-axis shows the abundance ($\log_2$) and the y-axis indicates the kernel density estimate of the probability density function.

(C) Correlation plots of three independent pooled screening replicates (R1, R2, and R3). The data shown are based on average normalized read counts.

(D) Differential representation of sgRNAs after cell expansion. Each dot indicates one gene ranked according to the relative sgRNA abundance (the $\log_2$ fold change) on day 8 versus day 0 (an average of four sgRNAs/gene in three biological replicate experiments). Blue dots indicate the top 20 genes corresponding to underrepresented sgRNAs at expansion day 8 (see main Figure 1D). FBXO11 is shown as a red dot. The yellow dot and arrow represent the average value of 19 control non–gene-targeting sgRNAs. See also Supplemental Table 3.

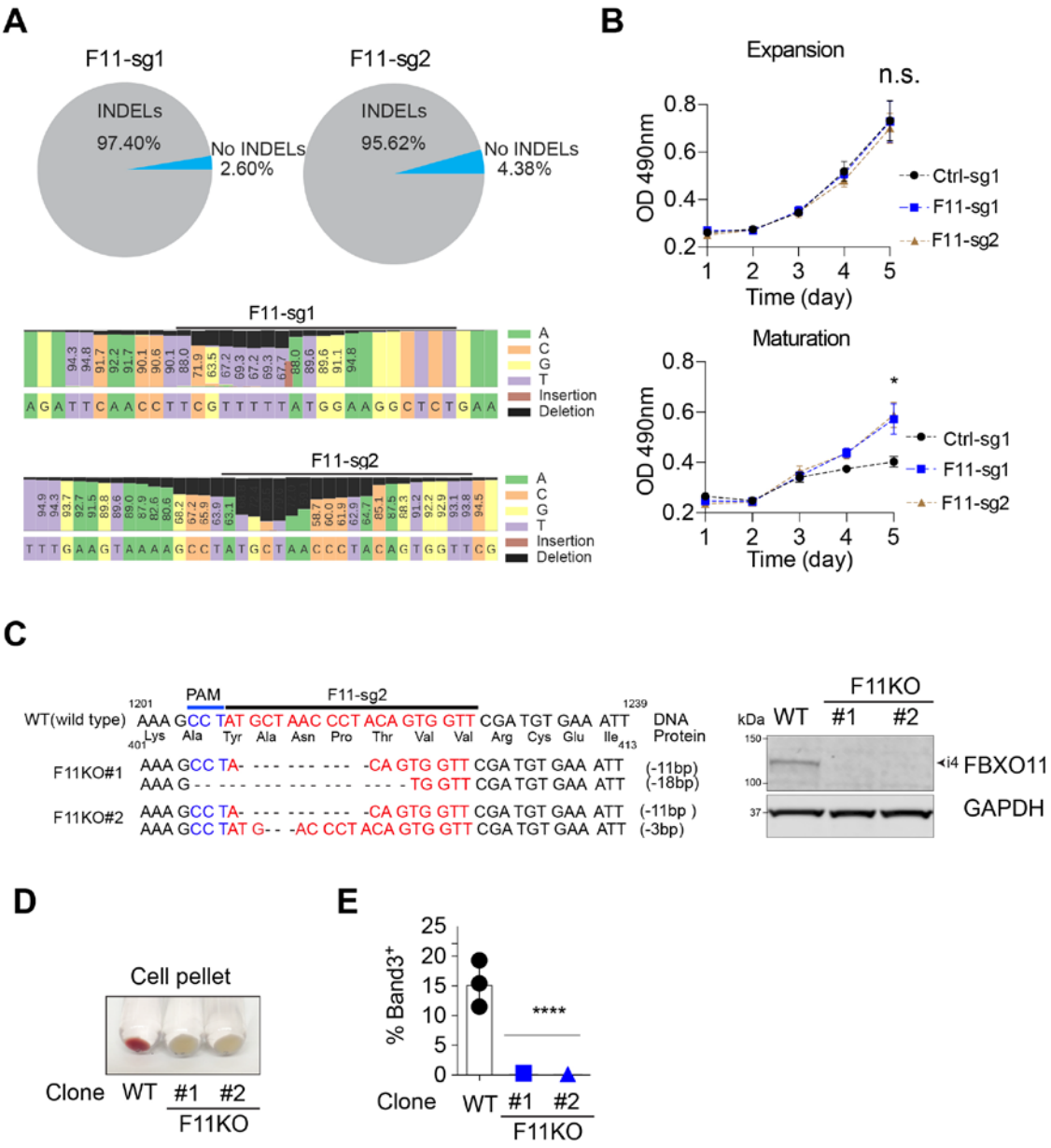

Supplemental Figure 2 (related to Figure 1). ***FBXO11*** **gene disruption inhibits erythroid maturation.** HUDEP-2 cells expressing Cas9 were transduced with a lentiviral vector encoding one of two different *FBXO11* sgRNAs and a puromycin resistance cassette. Transduced cells were selected by puromycin treatment and analyzed.

(A) INDEL fractions. The lower panels show the alignment of targeted deep-sequencing data in the genome-edited cell pools described in main Figure 1G–K. The black bars indicate deletions and the brown bars indicate insertions, with each nucleotide being represented by a different color.

(B) The growth of the Cas9 + sgRNA–expressing HUDEP-2 cell pools described in Figure 1G–K. Cells were grown in culture under conditions favorable for expansion (top graph) or maturation (bottom graph) for the number of days specified. Viable cell numbers were assessed by a colorimetric assay, with the light absorbance readout being shown on the y-axis. Note that immature cells expressing FBXO11 sgRNAs expanded normally (top graph) but did not undergo growth arrest during terminal maturation.

(C) Deletions in *FBXO11*-knockout (F11KO) HUDEP-2 cell clones generated with Cas9 + *FBXO11* sgRNA2. The sgRNA sequence is indicated in red and the PAM sequence in blue. Dashes indicate deleted nucleotides. Note that each clone is compound heterozygous for frameshift and in-frame mutations. The right panel shows Western blot analysis for FBXO11 protein. Arrow indicates the major isoform of FBXO11.

(D) Cell pellets at day 10 of induced maturation showing red color or lack thereof.

(E) Band3 expression (mean ± SEM) 5 days after induced maturation of WT and F11KO HUDEP-2 cell clones. ****$P < 0.0001$; unpaired *t*-test.

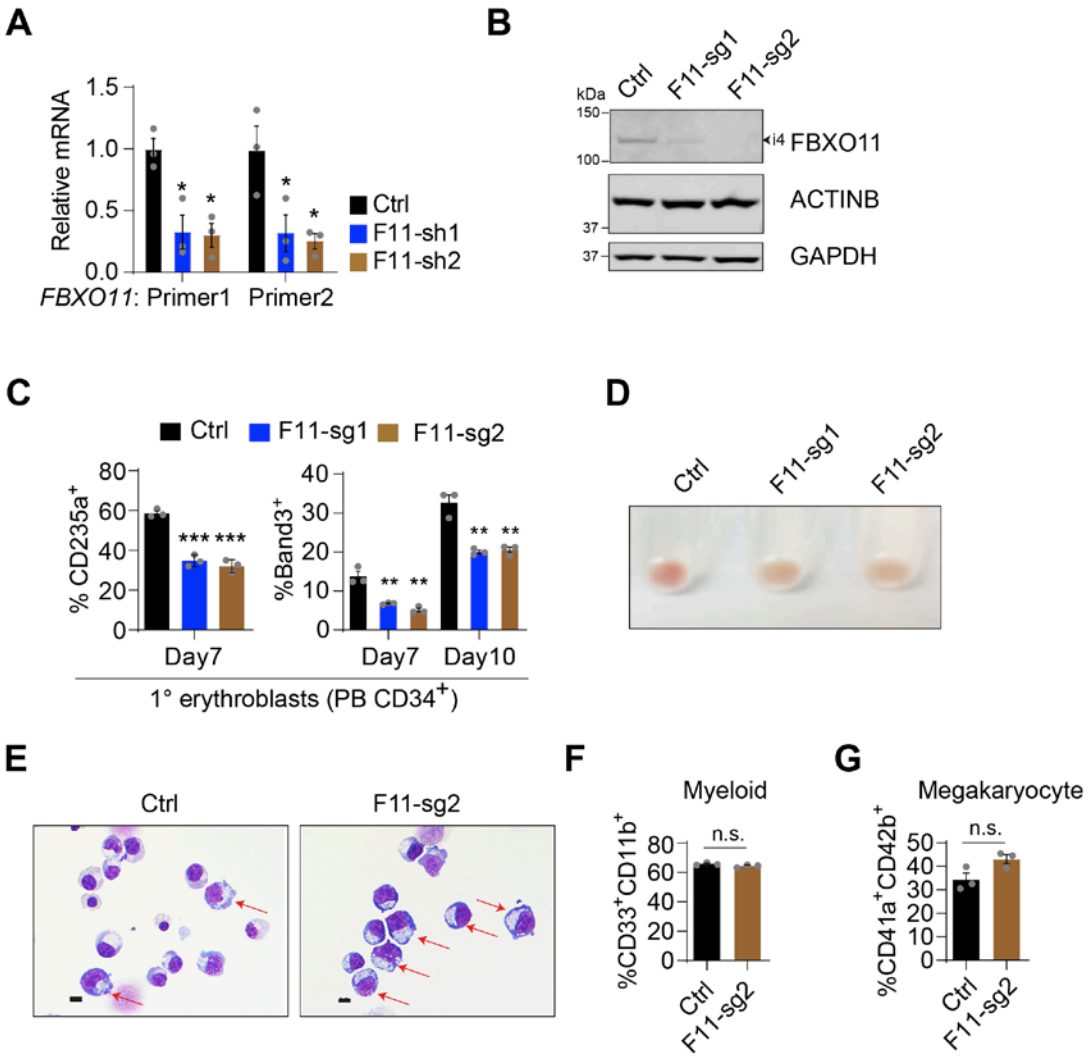

Supplemental Figure 3 (related to Figure 2). *FBXO11* disruption inhibits erythropoiesis in CD34⁺ hematopoietic stem and progenitor cells.

(A) Peripheral blood–mobilized human CD34⁺ cells were expanded for 2 days and then transduced with lentiviral vectors encoding GFP and *FBXO11* (F11-sh) or control (Ctrl) shRNAs, as described in main Figure 2A. Transduced (GFP⁺) cells were FACS-purified and grown in erythroid cytokines for 7 days, followed by measurement of *FBXO11* mRNA expression by quantitative real-time PCR amplification using two sets of distinct primers. The expression levels were normalized to *ACTB* mRNAs. The graph shows the results as the mean ± SEM for three biological replicate experiments.

(B–G) Peripheral blood (PB) mobilized CD34⁺ cells were expanded for 2 days, electroporated with Cas9 ribonucleoprotein complex containing non-targeting or *FBXO11* sgRNAs, and grown

in culture in medium to support erythroid (**B**–**E**) or multi-lineage hematopoietic (**F**, **G**) differentiation.

(B) Western blot showing FBXO11 protein expression at culture day 10 of erythroid culture. The arrow indicates the major isoform of FBXO11.

(C) The fraction of cells expressing CD235 (mean ± SEM) in three biological replicate experiments. ***$P < 0.001$; unpaired *t*-test. Band3 expression at days 7 and 10 (mean ± SEM for three biological replicates, right panel). **$P < 0.01$, ***$P < 0.001$; unpaired *t*-test.

(D) Cell pellets at culture day 10.

(E) May–Grünwald–Giemsa–stained erythroblasts at culture day 10. The red arrows indicate immature erythroblasts. The scale bar represents 10 μM.

(F) The expression of myeloid markers in day 10 cultures (mean ± SEM) from three independent experiments. The myeloid cultures included SCF, TPO, G-CSF, and GM-CSF. n.s., not significant; unpaired *t*-test.

(G) The expression of megakaryocyte markers in day 10 cultures (mean ± SEM) from three independent experiments. Products of megakaryocyte cultures included SCF, IL-6, IL-9, and TPO. n.s., not significant; unpaired *t*-test.

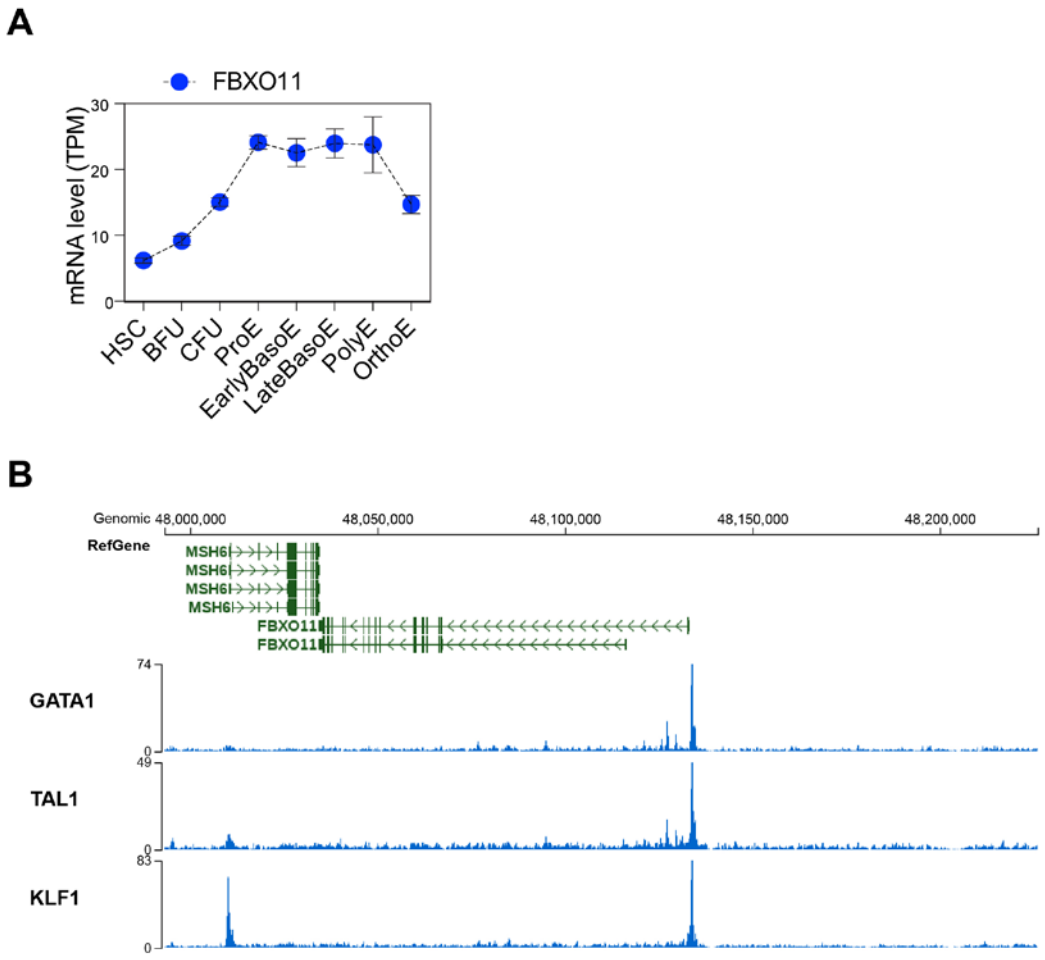

Supplemental Figure 4 (related to main Figure 2). The *FBXO11* gene is upregulated during human erythropoiesis and is bound by GATA1, KLF1, and TAL1.

(A) *FBXO11* mRNA expression during human erythropoiesis as determined by RNA sequencing at specific developmental stages (the x-axis). The y-axis shows the number of transcripts per kilobase million (TPM). The original data from a previous study were processed[1].

(B) Results of chromatin immunoprecipitation-sequencing analysis showing GATA1, KLF1, and TAL1 binding to the *FBXO11* promoter region in HUDEP-2 erythroblasts. The green line represents the *FBXO11* gene, with the exons being shown as rectangles. Transcription factor binding is shown in lower graphs.

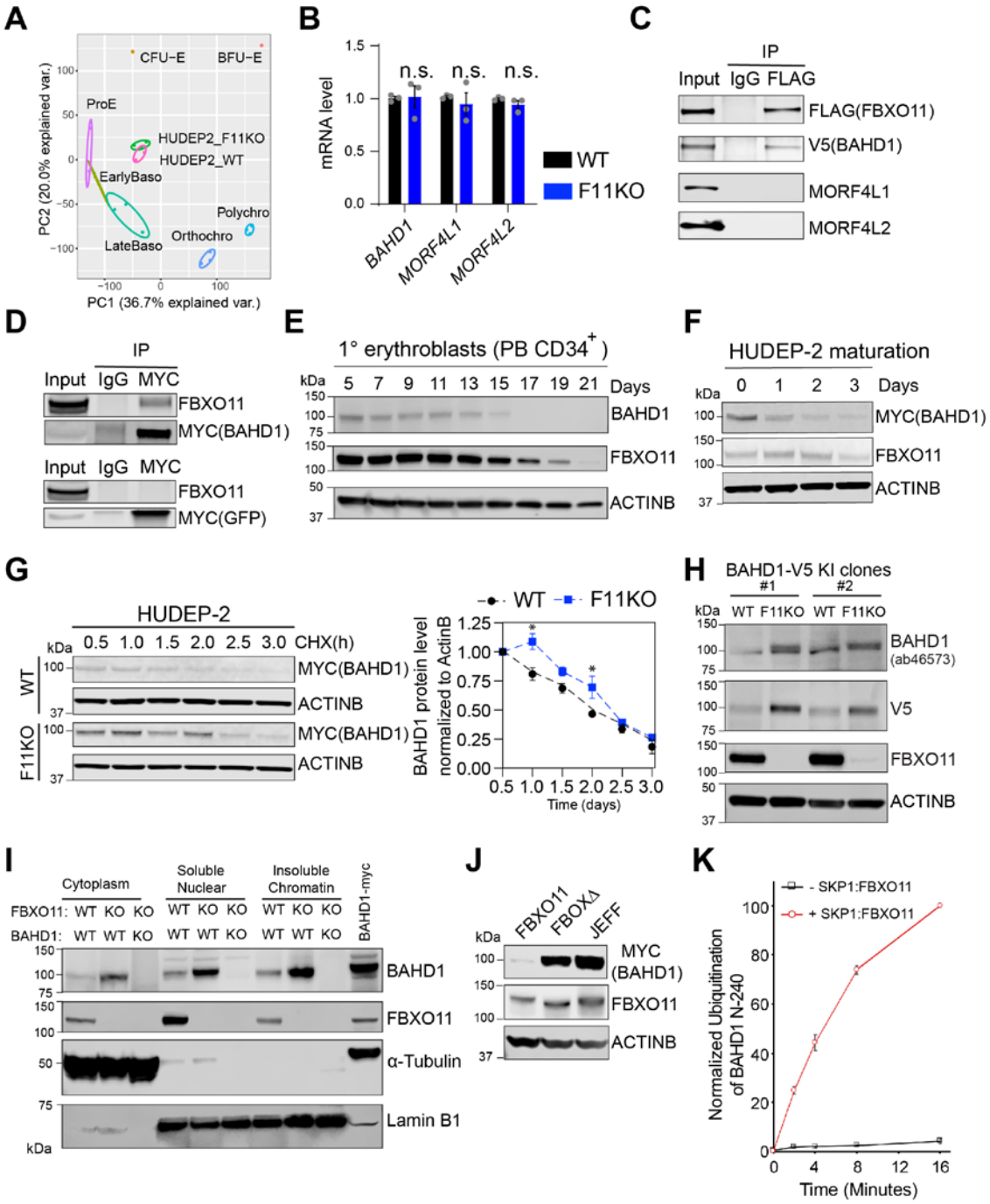

Supplemental Figure 5 (related to main Figure 3). FBXO11 destabilizes BAHD1 via direct binding and ubiquitination.

(A) Principal Component Analysis (PCA) of transcriptomes of WT and F11KO#2 HUDEP-2 cells (Supplemental Figure 2) cultured in expansion medium plotted with transcriptomes of human

$CD34^+$ cell–derived erythroid precursors at defined developmental stages[1]. The WT and F11KO#2 HUDEP-2 samples cluster together, indicating that they are from similar developmental stages.

(B) *BAHD1*, *MORF4L1*, and *MORF4L2* mRNA expression in WT and F11KO#2 HUDEP-2 cells (clone 2, Supplemental Figure 2) grown in culture in expansion medium. The graph summarizes the mean ± SEM from three biological replicate experiments. The values are normalized to *ACTB* mRNA. n.s., not significant; unpaired *t*-test.

(C) 293T cells were transfected with plasmids encoding FLAG–FBXO11 and BAHD1–V5. After 48 h, cell lysates were immunoprecipitated with anti-FLAG or IgG antibody and Western blot analysis was performed with the antibodies shown on the right. The input represents 10% of the immunoprecipitated samples.

(D) 293T cells were transfected with plasmids encoding BAHD1–MYC or GFP–MYC. After 48 h, cell lysates were immunoprecipitated with anti-MYC or IgG antibody and Western blot analysis was performed with the antibodies shown on the right. The input represents 10% of the immunoprecipitated samples.

(E) Western blot showing FBXO11 and BAHD1 protein expression during the maturation of human $CD34^+$ cell–derived erythroblasts.

(F) Western blot showing the kinetics of FBXO11 and BAHD1 protein expression during the induced maturation of HUDEP-2 cells overexpressing BAHD1–MYC.

(G) WT and F11KO#2 HUDEP-2 cells expressing BAHD1–MYC were treated with cycloheximide (50 μg/mL) and subjected to Western blot analysis over time. A representative Western blot is shown on the left. The graph shows the mean ± SEM BAHD1–MYC protein levels normalized to ACTINB in three biological replicate experiments. $*P < 0.05$; unpaired *t*-test.

(H) Western blot analysis of WT and F11KO HUDEP-2 clones expressing C-terminal V5-tagged BAHD1 from the modified endogenous gene.

(I) Western blot showing the expression of BAHD1 and FBXO11 proteins in different cellular compartments of clonal HUDEP-2 cell lines with WT and homozygous null (KO) alleles of *FBXO11* and/or *BAHD1*. The last lane represents the lysate from 293T cells expressing BAHD1–MYC.

(J) FBXO11 destabilizes BAHD1 in 293T cells. FBXO11–FLAG variants were expressed in 293T cells with BAHD1–MYC and subjected to Western blot analysis. WT, wild type; FBOXΔ, FBOX domain-deleted mutant; JEFF, Q491L mutant.

(K) Quantification of ubiquitination studies shown in main Figure 3I. Graph shows the mean ± SEM from 3 independent experiments are shown.

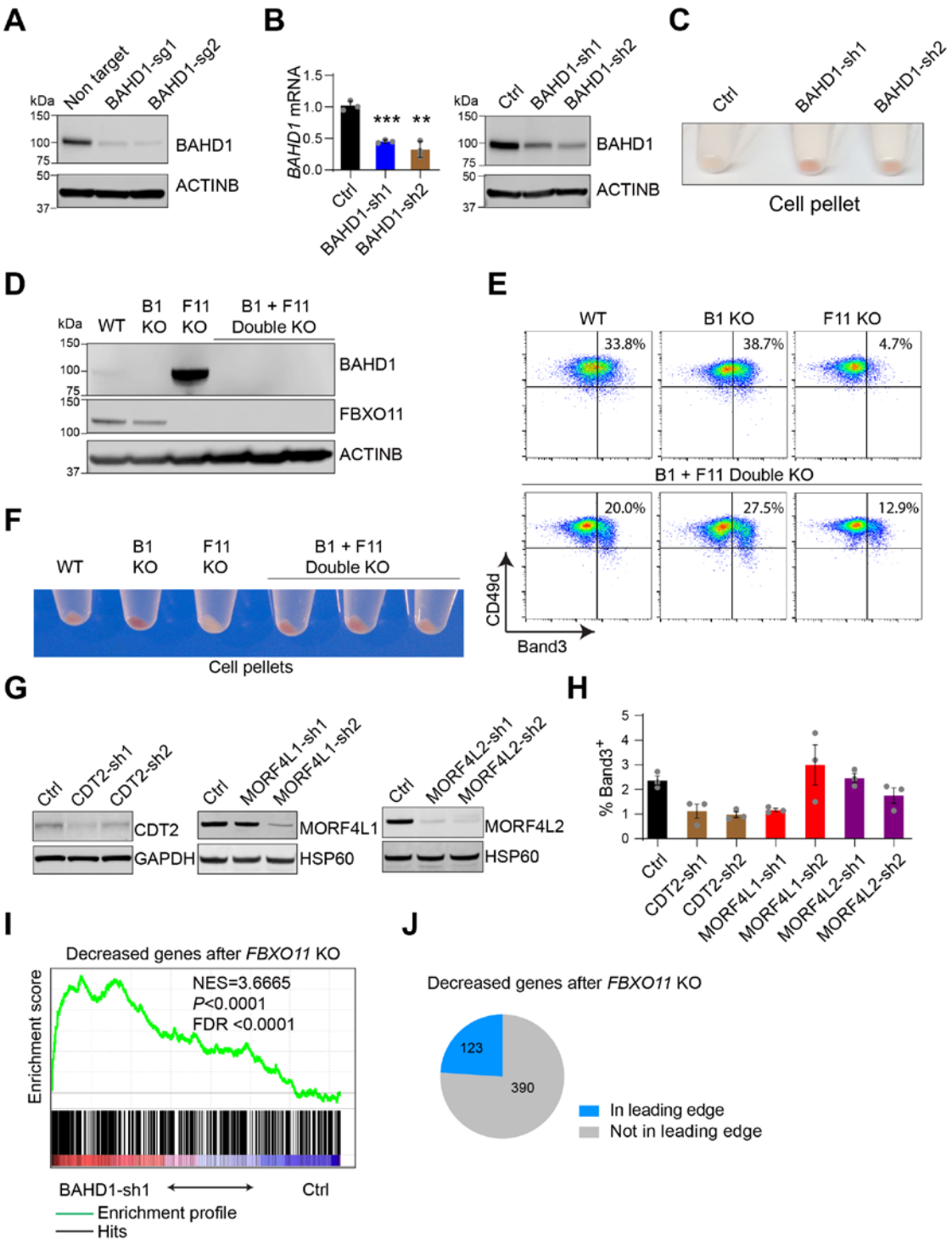

Supplemental Figure 6 (related to Figure 4). Suppression of BAHD1, but not of *CDT2*, *MORF4L1*, or *MORF4L2*, rescues erythroid maturation of *FBXO11* knockout HUDEP-2 cells.

(A) Western blot of BAHD1 in the *FBXO11*-knockout HUDEP-2 (F11KO#2) cell clone (Supplemental Figure 2) expressing *BAHD1* sgRNAs or a non-targeting sgRNA control.

(B) Real-time PCR and Western blot analysis of BAHD1 in F11KO#2 HUDEP-2 cells expressing BAHD1 or non-targeting control (Ctrl) shRNAs.

(C) Cell pellets in F11KO#2 HUDEP-2 cells expressing BAHD1 or non-targeting control (Ctrl) shRNAs at day 10 of induced maturation.

(D) Western blot analysis of BAHD1 and FBXO11 expression in clonal HUDEP-2 cell lines with the indicated genotypes. Mutant cell lines were generated by expressing *BAHD1* sgRNA2 in F11KO#2 clone.

(E) Band3 expression in WT, F11KO#2, and FBXO11/BAHD1–double-knockout HUDEP-2 cell clones after 5 days of induced erythroid maturation.

(F) Cell pellets of WT, F11KO#2, and FBXO11/BAHD1–double-knockout HUDEP-2 cell clones after 5 days of induced erythroid maturation.

(G) Western blot analysis of F11KO#2 cells expressing the indicated shRNAs.

(H) Expression of Band3 after 6 days of induced maturation of F11KO#2 cells expressing the indicated shRNAs. The graph summarizes the mean ± SEM $Band3^+$ cell fraction from three biological replicate experiments.

(I) Gene set enrichment analysis (GSEA) of differentially expressed mRNAs after *BAHD1* suppression in *FBXO11* KO HUDEP-2 cell, showing enrichment for a custom gene set of 513 transcripts that were reduced in *FBXO11* KO versus WT HUDEP-2 cells. NES, normalized enrichment score.

(J) Leading edge analysis of the decreased genes after *FBXO11* knockout that are significantly rescued by suppression of *BAHD1*. The pie charts show the mRNA transcripts that are significantly enriched (blue) or not significantly enriched (grey) in the custom gene set from GSEA analysis in panel **I**.

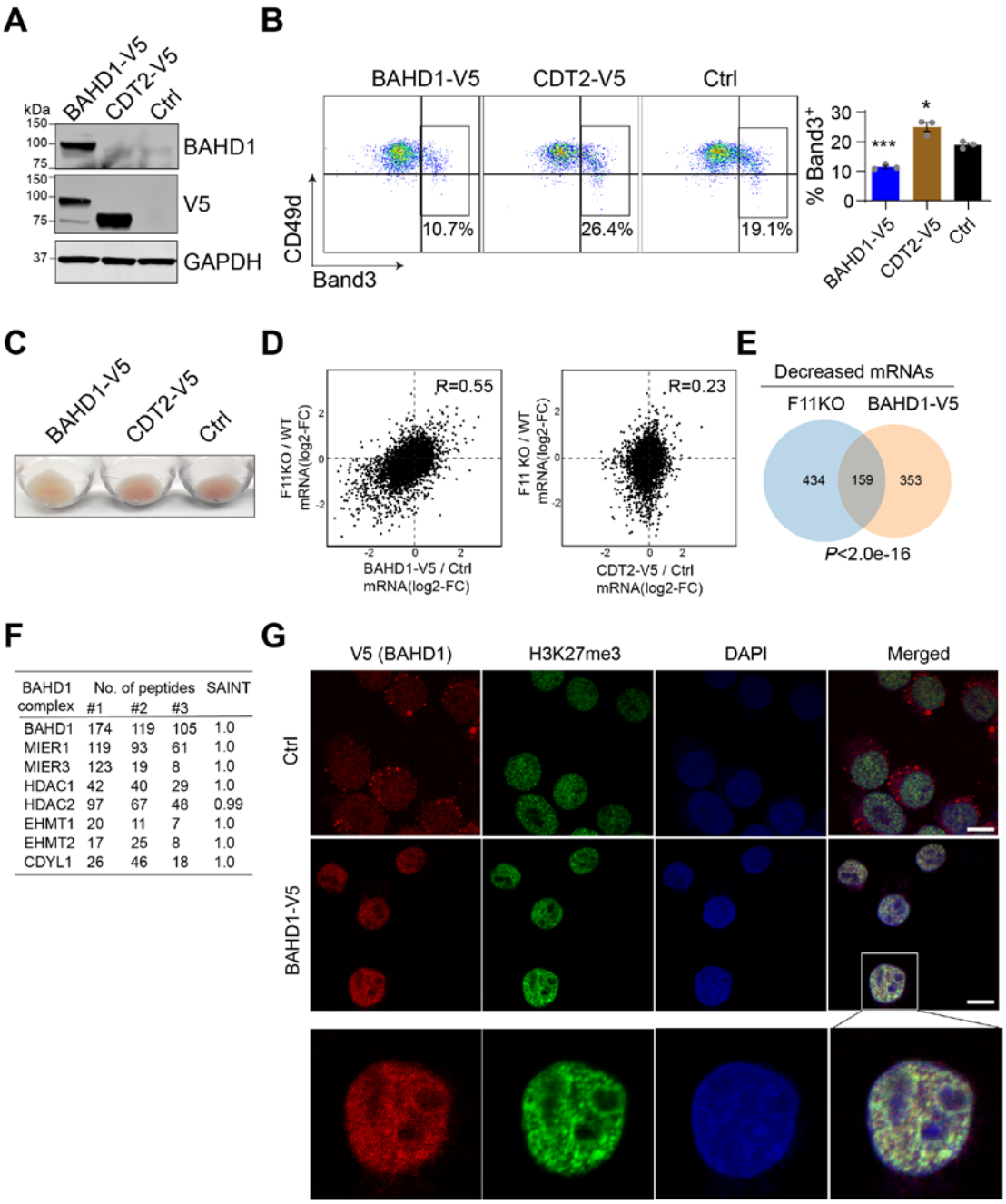

BAHD1 complex	No. of peptides #1	#2	#3	SAINT
BAHD1	174	119	105	1.0
MIER1	119	93	61	1.0
MIER3	123	19	8	1.0
HDAC1	42	40	29	1.0
HDAC2	97	67	48	0.99
EHMT1	20	11	7	1.0
EHMT2	17	25	8	1.0
CDYL1	26	46	18	1.0

Supplemental Figure 7 (related to Figure 4). Overexpression of BAHD1 recapitulates the effects of *FBXO11* knockout in HUDEP-2 cells.

(A) Western blot showing the expression of BAHD1 and CDT2 in HUDEP-2 cells overexpressing BAHD1–V5 or CDT2–V5 cultured under expansion conditions.

(B) Effects of enforced BAHD1–V5 or CDT2–V5 expression on Band 3 and CD49d expression in HUDEP-2 cells after 3 days of induced maturation. Representative flow cytometry plots are shown at left. The graph shows the mean ± SEM Band3 expression in three biological replicate

experiments. Ctrl denotes control cells transduced with empty vector. ***$P < 0.001$; unpaired *t*-test.

(C) Cell pellets at day 3 of induced maturation in HUDEP-2 cells overexpressing BAHD1–V5, CDT2–V5, or control (Ctrl) vector.

(D) RNA-seq analysis of HUDEP-2 cells with the indicated genotypes cultured under expansion conditions. The left panel compares the RPKM fold-change in 14,313 transcripts after *FBXO11* knockout (KO) (y-axis) to the fold-change after BAHD1–V5 overexpression (x-axis). The right panel shows a similar analysis after overexpression of CDT2–V5. R, correlation coefficient.

(E) Overlap between mRNA transcripts that are decreased in HUDEP-2 cells after *FBXO11* knockout or BAHD1–V5 overexpression ($\log_2$ fold change ≤ 1.0, $P < 0.05$). The *P* value was determined by Fisher's exact test.

(F) Lysates from HUDEP-2 cells expressing BAHD1–V5 were immunoprecipitated with V5 antibody then subjected to mass spectroscopy analysis. The numbers of peptides identified in three independent experiments are summarized. A significance analysis of interactome (SAINT) score greater than 0.9 indicates strong interaction[2].

(G) Immunofluorescence images showing immunostaining with antibodies to V5 and H3K27me3 in HUDEP-2 cells overexpressing BAHD1–V5 and wild type control cells. Scale bar, 10 μM. Bottom panels show a three-fold magnification of the images shown in the second row.

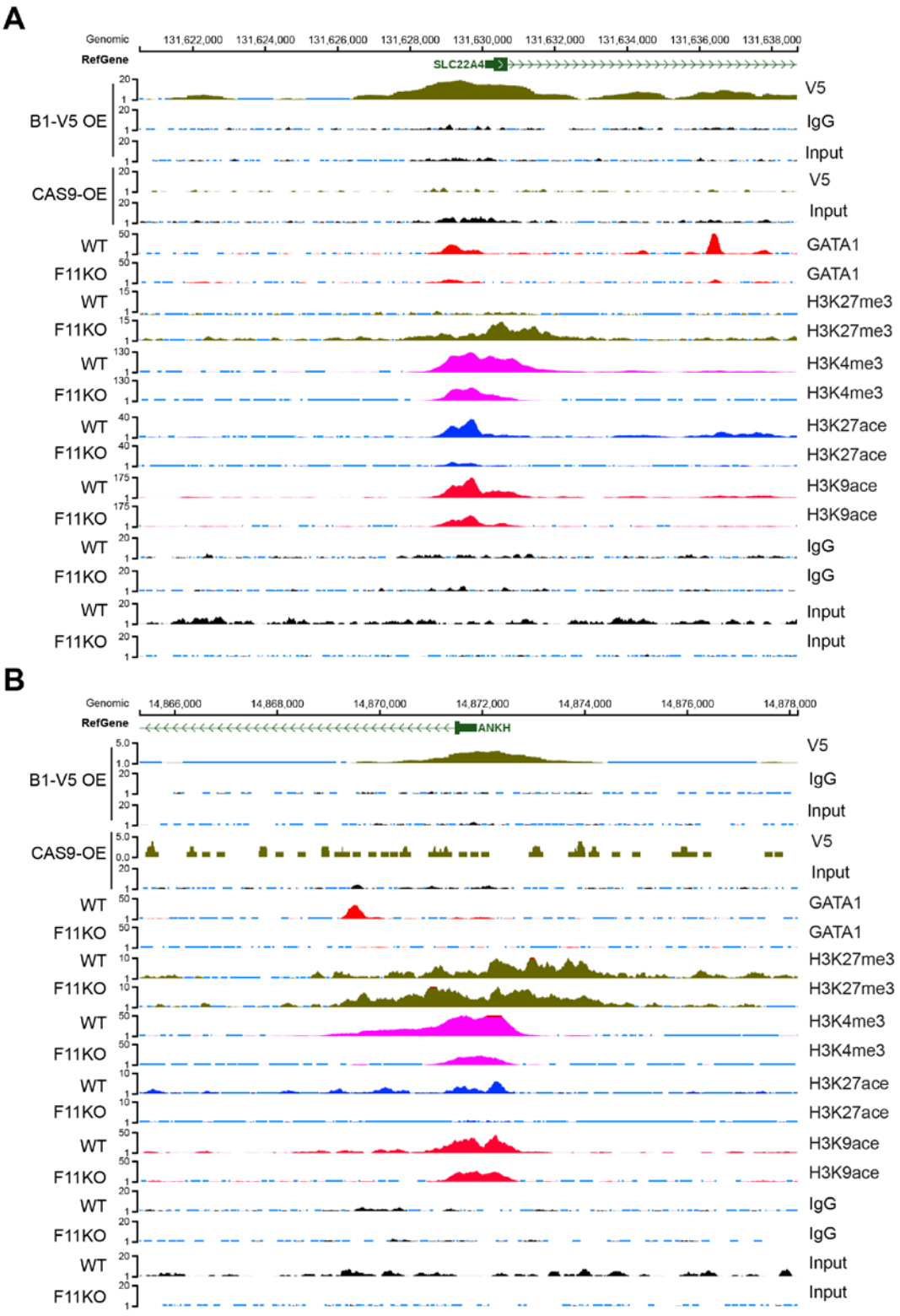

Supplemental Figure 8 (related to Figure 5). Epigenetic analysis of two erythroid genes that are downregulated after loss of FBXO11 in HUDEP-2 cells.

Representative ChIP-seq data near the TSS of *SLC22A4* (A) and *ANKH* (B) genes. The ChIP-seq results for H3K27me3, H3K4me3, GATA1, H3K27ace, and H3K9ace were determined in WT and *FBXO11*-knockout HUDEP-2 cells (F11KO clone #2). The ChIP-seq results for BAHD1–V5 (B1-V5) were determined separately in HUDEP-2 cells engineered to express the epitope-tagged protein and CAS9-overexpressing (OE) control cells. IgG and Input DNA were analyzed as negative controls for each experiment.

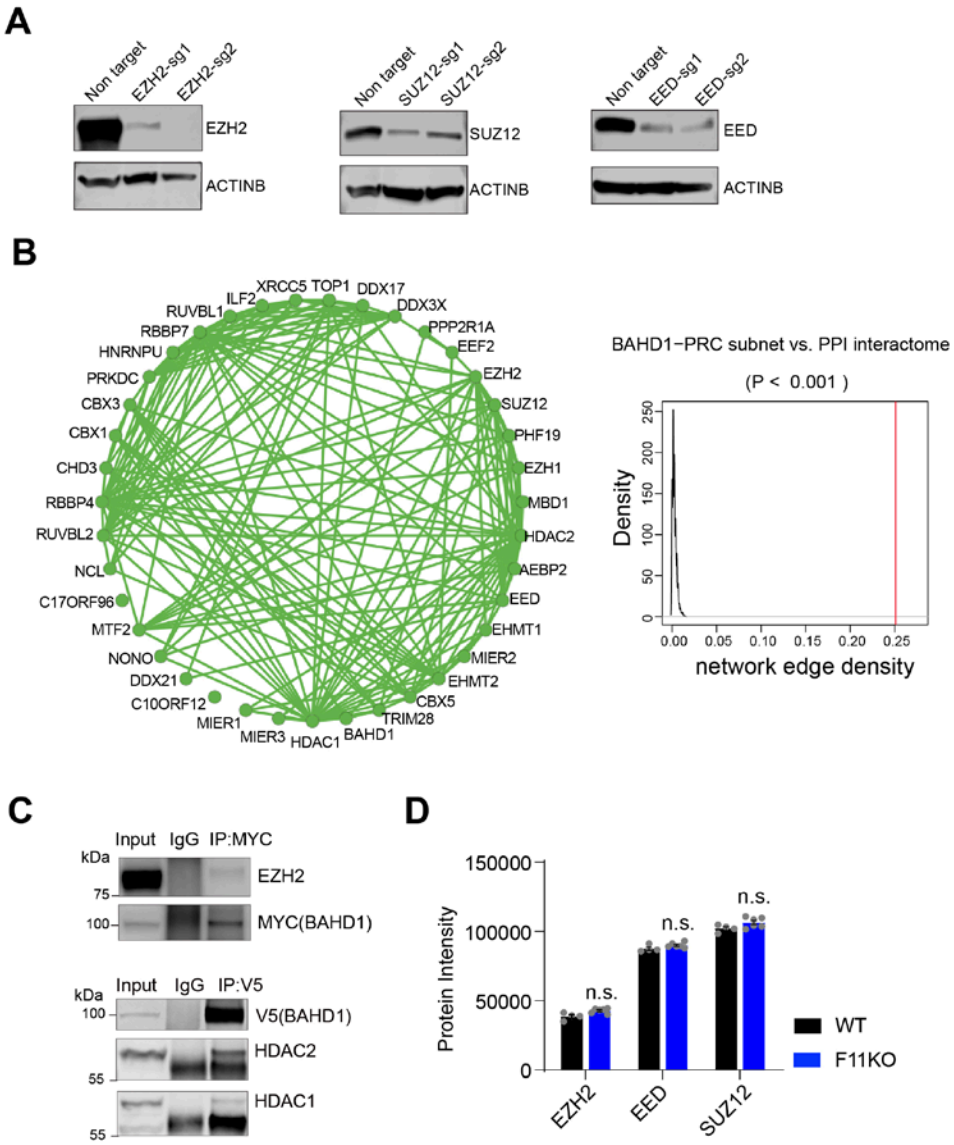

Supplemental Figure 9 (related to Figure 6). BAHD1 interacts functionally and physically with the PRC2 complex

(A) Western blot showing EZH2, EED, and SUZ12 expression in *FBXO11*-knockout HUDEP-2 cells (clone F11KO#2, Supplemental Figure 2) expressing Cas9 and the indicated sgRNAs or control (Ctrl) sgRNA.

(B) Protein network analysis of the PRC2 complex and BAHD1 complex (see also the Methods section). The BAHD1−PRC subnetworks are densely connected, with the connectivity (network edge density) being significantly higher than that of random subnetworks (permutation test $P < 0.001$).

(C) Lysates from WT HUDEP-2 cells stably expressing BAHD1–MYC were immunoprecipitated with anti-MYC antibody then analyzed by Western blotting for the PRC2 component EZH2. The input lanes represent 10% of the immunoprecipitated sample. Lysates from HUDEP-2 cells expressing BAHD1–V5 were immunoprecipitated with anti-V5 antibody (or IgG control) then subjected to Western blot analysis with the known BAHD1-interacting proteins HDAC1 and HDAC2.

(D) Expression of the PRC2 components EZH2, EED, and SUZ12 in WT and F11KO HUDEP-2 cells. The graphs show the mean ± SEM of the protein intensity from quantitative proteomics. n.s., not significant; unpaired *t*-test.

References

1. An X, Schulz VP, Li J, et al. Global transcriptome analyses of human and murine terminal erythroid differentiation. *Blood*. 2014;123(22):3466–3477.
2. Choi H, Larsen B, Lin ZY, et al. SAINT: probabilistic scoring of affinity purificationg-mass spectrometry data. *Nat. Methods*. 2011;8(1):70–73.

Supplemental Table Legends (separate files)

Supplemental Table 1. Single-guide (sg) RNAs targeting ubiquitin–proteasome system components. Columns are labeled as follows: A, gene ID; B, gene symbol; C, sgRNA target sequence; D, corresponding target transcript ID; E, sgRNA-targeted exon.

Supplemental Table 2. Representation of sgRNAs in immature (Band3^{-}) versus mature (Band3^{+}) HUDEP-2 cells after 5 days of erythroid maturation. Columns are labeled as follows: A, gene name; B, average fold change of sgRNA in Band3^{+} versus Band3^{-} cells; C, *P* value from three independent replicate experiments. Significant hits were also called from MAGeCK and the enriched GO pathway from EnrichR (listed as a separate sheet).

Supplemental Table 3. Representation of sgRNAs in immature HUDEP-2 cells after 8 days of expansion. Columns are labeled as follows: A, gene name; B, average fold change of sgRNA in Band3^{+} versus Band3^{-} cells; C, *P* value from thee independent replicate experiments. Significant hits were also called from MAGeCK and enriched GO pathway from EnrichR (listed as a separate sheet).

Supplemental Table 4. Integrative analysis of RNA-seq and TMT proteomics in WT and pooled *FBXO11* knockout (F11KO) HUDEP-2 erythroblasts cultured under expansion conditions. Columns are named as follows: A, gene name; B, gene name; C and D, $\log_2$ fold change in the mRNA expression level from RNA-seq and corresponding *P* value; E and F, $\log_2$ fold change of protein level and *P* value from TMT proteomics. Potential substrates as outliers from the linear regression model are shown in a separate tab.

Supplemental Table 5. RNA transcriptome analysis of *FBXO11* knockout HUDEP-2 cells (F11KO#2, supplemental Figure 2C) expressing *BAHD1* shRNAs (shRNA1 in tab1 and shRNA2 in tab2) or control (luciferase) shRNA grown in culture under maturation conditions for 6 days. Columns are named as follows: A, gene name; B, $\log_2$ fold change in mRNAs in F11KO#2 HUDEP-2 cells expressing *BAHD1* sh1 or sh2, versus shLuc; C, average expression of genes (RPKM) in shLuc cells; D, E, and F, *t*-test results as *t* value, *P* value and adjusted *P* value. Decreased genes after *FBXO11* knockout that are significantly rescued by suppression of *BAHD1* and analyzed by GSEA leading edge analysis are shown in a separate tab 3.

Supplemental Table 6. RNA transcriptome analysis of HUDEP-2 cells expressing BAHD1–V5 versus empty vector control (Ctrl) grown under expansion conditions. Columns are named as follows: A, gene name; B, $\log_2$ fold change in expression level in BAHD1–V5 versus control (Ctrl) cells; C average gene expression (RPKM) in Ctrl cells. Columns D, E, and F, *t*-test results as *t* value, *P* value, and adjusted *P* value.

Supplemental Table 7. RNA transcriptome analysis of HUDEP-2 cells expressing CDT2–V5 or empty vector control (Ctrl) grown under expansion conditions. Columns are named as follows: A, gene name; B, $\log_2$ fold change in expression level in CDT2–V5 versus control (Ctrl) cells; C, average gene expression (RPKM) in Ctrl cells. Columns D, E, and F, *t*-test results as *t* value, *P* value, and adjusted *P* value.

Supplemental Table 8. Histone marks in BAHD1–V5 binding regions of FBXO11-regulated genes in *FBXO11* knockout and WT HUDEP-2 cells grown under expansion conditions. Columns are named as follows: A, chromatin coordination; B, gene category based on expression change after *FBXO11* knockout, KO7.down represents decreased genes KO7.up represents increased genes and KO7.control represents unchanged genes in *FBXO11* KO#2 HUDEP-2 cells; C, enrichment fold change of H3K27me3 marks in *FBXO11* knockout versus WT cells; D, enrichment fold change of H3K4me3 marks in *FBXO11* knockout versus WT cells; E, annotated nearest gene name.

Supplemental Table 9. BAHD1–V5–bound genes in BAHD1–V5 HUDEP-2 cells grown under expansion conditions. Peaks were called according to the parameter described in Supplemental Methods Page 14.

Supplemental Table 10. Analysis of CRISPR screen using single-guide (sg) RNAs targeting epigenetic modifiers. Tab1 shows genes represented by corresponding sgRNAs that are differentially expressed in Band3^{+} vs. Band3^{-} *FBXO11* KO#2 HUDEP-2 cells after induced maturation. Columns are labeled as follows: A, gene name; B, average fold change of sgRNA in Band3^{+} versus Band3^{-} cells. Genes representing PRC2 subunits are highlighted. The second tab is the original sgRNA library sequence information, NGS count indicates the coverage of sgRNA from original plasmids for quality control.

Supplemental Table 11. Oligonucleotides (tab 1), DNA primers (tab 2), and antibodies (tab 3) used in this study. Oligonucleotides were used for sgRNA or shRNA vector construction; DNA primers were used for the analysis of Cas9-mediated indels by Sanger sequencing or NGS deep sequencing; antibodies were used for Western blotting, immunoprecipitation, or ChIP-seq analysis.